Available online at www.sciencedirect.com
ScienceDirect
Earth and Planetary Science Letters 257 (2007) 121–131
EPSL
www.elsevier.com/locate/epsl

# Cryogenic opal-A deposition from Yellowstone hot springs

Alan Channing [a,*], Ian B. Butler [b,1]

[a] School of Earth, Ocean and Planetary Sciences, Cardiff University, PO Box 914, Cardiff, Wales, CF10 3YE, UK
[b] School of GeoSciences, The University of Edinburgh, Grant Institute, The King's Buildings, West Mains Road, Edinburgh, Scotland, EH9 3JW, UK

Received 19 December 2005; received in revised form 14 February 2007; accepted 15 February 2007
Available online 23 February 2007
Editor: H. Elderfield

**Abstract**

Sub-zero winter temperatures on the Yellowstone Plateau alter the opal-A precipitation pathway of fluid erupting from hot springs and geysers. Frozen fluid, often only meters from boiling pools, contains abundant opal-A particles, comprising sheet and filament-like aggregations of opal-A microspheres which are formed by opal-A precipitation in brine pockets, channels and veins by natural cryogelling. Unconsolidated cryogenic opal-A sediment accumulates in and below water-ice where it is locked until spring thaw conditions. Sediment is then either remobilized, contributing large volumes of opal-A particulate to geothermally influenced wetlands, or becomes adhered, *in situ*, by dehydration and cementation. This strongly seasonal opal-A precipitation regime has been overlooked in investigations of sinter deposition, accretion rates and microbe/mineral interactions. Natural opal-A textures recorded from Yellowstone may be replicated simply by freezing and thawing synthetic silica–salt solution in the laboratory. Cryogenic process may have influenced mineral precipitation and sediment accumulation in many other geothermal areas. Particularly, active terrestrial springs located at high altitude/latitude, fossil systems influenced by ancient glaciations, plus potential astrobiological targets e.g. Mars and Europa.
© 2007 Elsevier B.V. All rights reserved.

*Keywords:* Yellowstone; geochemistry; silica; opal; hot spring

## 1. Introduction

Yellowstone's geothermal basins are utilized as analogues for ancient [1,2] and possible extraterrestrial counterparts [3–5] in research to establish criteria for recognizing biogenic signatures in hot spring deposits [6]. Interpretations of silica deposition, sinter formation and microbial fossilization in and around the hot springs and geysers of Yellowstone have been based on processes observed during the late-spring, summer and early autumn ([7,8] but see [9]). Here we describe silica deposition during the Yellowstone winter, when geothermal fluids flow into a sub-zero environment where erupted-waters freeze. We describe cryogenic silica precipitation that produces unconsolidated opal-A sediment within and beneath geothermal water-ice, which illustrates a dichotomy between winter and summer opal-A precipitation pathways.

### 1.1. Yellowstone National Park

Yellowstone National Park, Wyoming, USA, has Earth's largest concentration of terrestrial hot springs

* Corresponding author.
*E-mail address:* channinga@cardiff.ac.uk (A. Channing).
[1] ECOSSE (Edinburgh Collaborative of Subsurface Science and Engineering). A Joint Research Institute of the Edinburgh Research Partnership in Engineering and Mathematics.

0012-821X/$ - see front matter © 2007 Elsevier B.V. All rights reserved.
doi:10.1016/j.epsl.2007.02.026

and geysers, which are associated with the ~600 Ka Yellowstone Caldera and the Norris–Mammoth Corridor graben system [10]. Major areas of geothermal activity occur at Norris, Lower, Midway, Black Sand and Upper Geyser Basins (Supplementary data Fig. 1), located on a series of plateaus at an altitude of ~2500 m. Local climate is characterized by long, cold winters and short, cool summers (Supplementary data Table 1a). Daily maximum air temperatures generally remain below freezing between November and March (Supplementary data Table 1b).

The reduced atmospheric pressure of the Yellowstone Plateau dictates that water boils at 93 °C, whilst during extreme cold conditions air temperatures are as low as −35 °C. Geothermal gradients at the margins of a hot spring pool and its sinter apron can span 128 °C over <1 m. Almost half of annual precipitation falls during the winter as snow curtailing hydrodynamic sediment transport until the spring thaw.

### 1.2. Opal-A deposition during summer conditions

Fluids emanating from the geothermal features at Yellowstone generally have an alkali-chloride (ca. 470 ppm $Na^{+}_{(aq)}$; ca. 450 ppm $Cl^{-}_{(aq)}$), high silica (up to 750 ppm $SiO_{2(aq)}$), character and are derived at depth in the geothermal system by the interaction of meteoric water with acid-intermediate volcanic rocks [10]. Geothermal waters up-welling into and erupting from hot spring vent pools cool and become supersaturated with respect to opaline silica, which promotes opal-A nucleation. Where high pH and low salt concentrations prevent aggregation, nuclei grow via Ostwald ripening into nanospheres and microspheres (diameter ca. 10 nm − 1 μm). If pH/electrolyte concentrations remain favourable and/or when fluid turbulence maintains particle-dispersion, colloidally-stable particle-suspensions (sols) form. As microspheres grow to exceed colloidal dimensions sol stability collapses and they sediment from suspension [11]. Hot spring pools containing opal-A sols appear milky-blue as sunlight is scattered by suspended microspheres [12]. Whilst within colloidal dimensions, deposition of opal-A microspheres from a sol is effected as chemical and physical conditions in the enclosing medium change. A lowering of pH or an increase in electrolyte concentration encourages particle aggregation via flocculation (where microspheres are strongly attracted) and coagulation (where microspheres remain weakly repelling) [13]. Interparticle collisions may be encouraged where microspheres are forced together via physical removal of the aqueous medium (e.g. by evaporation) in the process of gelation. Particle aggregation progresses to a point where sedimentation occurs [13]. In sub-aqueous environments such as vent pools or sinter terrace pools particle growth and particle aggregation are the dominant sedimentation processes, whilst gelation is predominant in drying sub-aerial environments such as sinter aprons.

Silica deposited in summer conditions forms well documented sub-aqueous and sub-aerial sinter deposits that are hard, structurally robust and relatively immobile. Silica precipitation from erupted fluid commonly occurs *in situ* on microbes, creating microbially influenced mineral fabrics including columnar and stratiform stromatolites, botryoids, spicules, shrubs, streamers and palisades [6–8,14,15]. The durability of these precipitates is evidenced by their presence in the fossil record where they provide morphological marker fabrics of former hot spring and biological activity [1,2]. Silica deposited during the Yellowstone summer is rich in distinctive biological silica precipitates such as diatom tests. Despite the dominance of published studies of summer deposition, the climate regime at Yellowstone dictates that a great proportion of the yearly output of geothermal fluid is erupted into a freezing environment.

## 2. Methods

### 2.1. Natural silica materials

Natural cryogenic sediment was collected from Opalescent Hot Spring, Porkchop Geyser and Big Blue Hot Spring at Norris Geyser Basin and Ear Spring and Sawmill Geyser at Upper Geyser Basin. At all springs, except Sawmill Geyser, sediment was collected from sinter surfaces below or at the margins of melting geothermal water-ice. At Sawmill sediment was collected from an ice cone forming on a boardwalk elevated above the sinter apron.

Mineral phases present were identified with a Phillips PW1710 analytical powder X-ray diffractometer (XRD), using CuKα radiation. Sediment samples were prepared for scanning electron microscope (SEM) observation by mounting on Al stubs with carbon pads and sputter-coating with gold/palladium. Observation and imaging were conducted with the secondary electron (SE) detector of a Phillips XL30 environmental SEM (ESEM), [accelerating voltage − 20 keV, working distance 5–10 mm]. Additional sediment samples were mounted either on Al stubs with carbon pads, or in a platinum crucible and left uncoated for qualitative elemental composition analyses. These were conducted with the gas secondary electron detector of the Phillips

XL30 ESEM [accelerating voltage 20 keV, working distance 10 mm] in combination with an Oxford Instruments, Link System EDX spectrometer and Link ISIS, Inca analytical software.

### 2.2. Cryogenic opal-A synthesis

All reagents were of analytical grade and used without further purification. Solutions were prepared with 0.22 μm filtered; 18.2 MΩ cm deionised water. A simple synthetic geothermal fluid in the form of a 450 ppm aqueous solution of silica was prepared using $Na_2SiO_3 \cdot 5H_2O$ and the pH adjusted to pH 6.5 by dropwise titration with HCl to produce a silica and sodium chloride solution. No silica precipitation occurred during pH adjustment. The synthetic fluid was frozen at −20 °C overnight. Freezing rates and direction were not controlled in these experiments as they are not controlled in equivalent natural environments. Synthetic opal-A was recovered after thawing at room temperature by filtration on a 0.02 μm Anodisc 47 membrane filter and washed with deionised water to remove residual NaCl. The product was air-dried and analysed using the instruments and techniques outlined above.

## 3. Results

### 3.1. Environments of opal-A sediment accumulation

Unconsolidated cryogenic opal-A sediments are common and widespread in the geyser basins of Yellowstone during winter and accumulate in a variety of environments, e.g. on sinter apron (Fig. 1a–j, Supplementary data Fig. 2c–g) and geothermally influenced wetland (Fig. 1d) surfaces and in dormant vent pools (Supplementary data Fig. 2a–b). A visual inventory of springs in the Norris and Upper Geyser Basins in February 2000 revealed opal-A sediments associated with the majority of alkali-chloride springs. Two geothermal features, a sporadically erupting geyser and a sporadically erupting spring, are selected here to illustrate typical environments of sediment formation and accumulation. Ice and sediment formation occurred during the preceding four-month period against the climatic background summarized in Supplementary data Table 1b.

Ear Spring, Upper Geyser Basin (Fig. 1a), is a boiling alkali-chloride spring with recorded vent temperature ~93 °C, pH 8.76 and conductivity 1270 μS/cm [16]. The spring has surging eruptions typified by filling and overflowing of the vent pool [17]. In summer erupted water flows through a short (~1 m long) run-off channel and across a narrow sinter apron with proximal microbial mats and a brecciated sinter surface laterally and distally. Water flows across the sinter apron as a broad shallow sheet (Fig. 1b) and eventually ponds or sinks in a shallow wetland depression (Fig. 1d). During observation in February 2000, the spring was characterized by vigorous boiling within the vent but little discharge (Fig. 1a–b). Areas of the sinter apron beyond the short run-off channel were covered with a ca. 2 cm thick ice-sheet (Fig. 1b). At the lateral ice-sheet margins melt-back was depositing fresh, bright-white opal-A sediment on and within the brecciated sinter surface as positive peaks and ridges up to ca. 1 cm high and as mm-cm thick lenses within shallow depressions (Fig. 1c). At the distal end of the frozen run-off, in the shallow wetland depression, an ice-sheet ca. 1–3 cm thick covered water standing above a bright-white powdery opal-A sediment, sufficiently thick (ca. 1–2 cm) to bury the basal regions of plants (Fig. 1d).

Ice cones are common features associated with many alkali-chloride geysers during winter conditions (e.g. 10,17]). Sawmill Geyser, Upper Geyser Basin (Fig. 1e) is a fountain-type geyser which erupts for a duration of 15–90 min to a height of 1.5–12 m, at an interval of 1–3 h. Fluid within the vent pool has a temperature of 88–97 °C [17]. During February 2000 areas of boardwalk adjacent to Sawmill Geyser (Fig. 1f) were covered with a substantial accumulation of clear-blue ice which had been deposited when spray from the geyser had landed on the boardwalk which is isolated from the thermal ground below. Enclaves of opaque opal-A precipitate (often >1 cm diameter) randomly distributed within the ice matrix formed a major component (10–20% by volume, visual estimate) of the deposit (Fig. 1g,h). Partial melting had liberated sediment which coated the boardwalk (Fig. 1i) and adjacent sinter substrates, in places to a depth of 1–2 cm. Micro-terraces and channels visible on sediment surfaces indicate periods of sediment mobility following deposition (Fig. 1j). Melt depressions in the ice surface contained small volumes of liquid water and lenses of opal-A sediment.

### 3.2. Sediment and particle morphology and composition

Natural and synthetic sediment exhibit a broad Bragg reflection (Supplementary data Fig. 3a) characteristic of opal-A [18]. Natural (Fig. 2a–j) and synthetic (Fig. 2k–s) precipitates contain micron to millimetre scale aggregates comprising densely packed

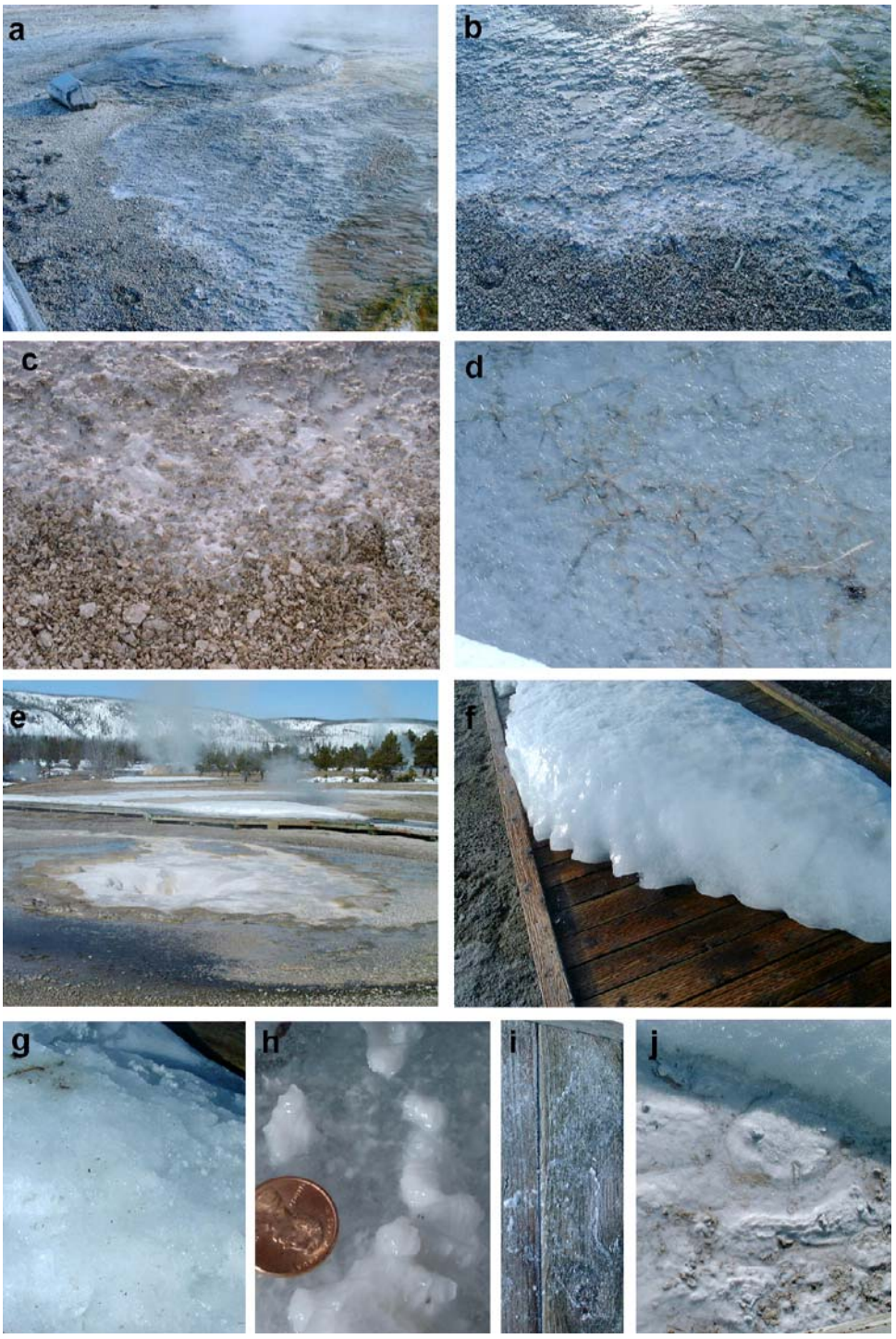


Fig. 1. Ice and cryogenic opal-A sediment associated with geothermal features, Yellowstone N. P. Ear Hot Spring, February 2000 (a–d) Boiling vent pool (a) with geothermal ice (b) formed less than a metre from the vent outflow. Silica sediment (c) liberated from ice by melting of the lateral margin infills relief in sinter chip breccia. Distal region of run-off (d), with ice formed above liquid water. Wilted plants are becoming buried by cryogenic opal-A sediment accumulation. Sawmill Geyser, February 2000 (e–j). Sawmill Geyser (e) vent (foreground) and geothermal ice cone (on boardwalk). Ice accretion is favoured on the boardwalk which is isolated from the thermal ground below (f). Ice cone contains enclaves of opal-A sediment (f–h) which accumulates on (i) and below (j) boardwalk following melting. Sediment mobility is indicated by channelling.

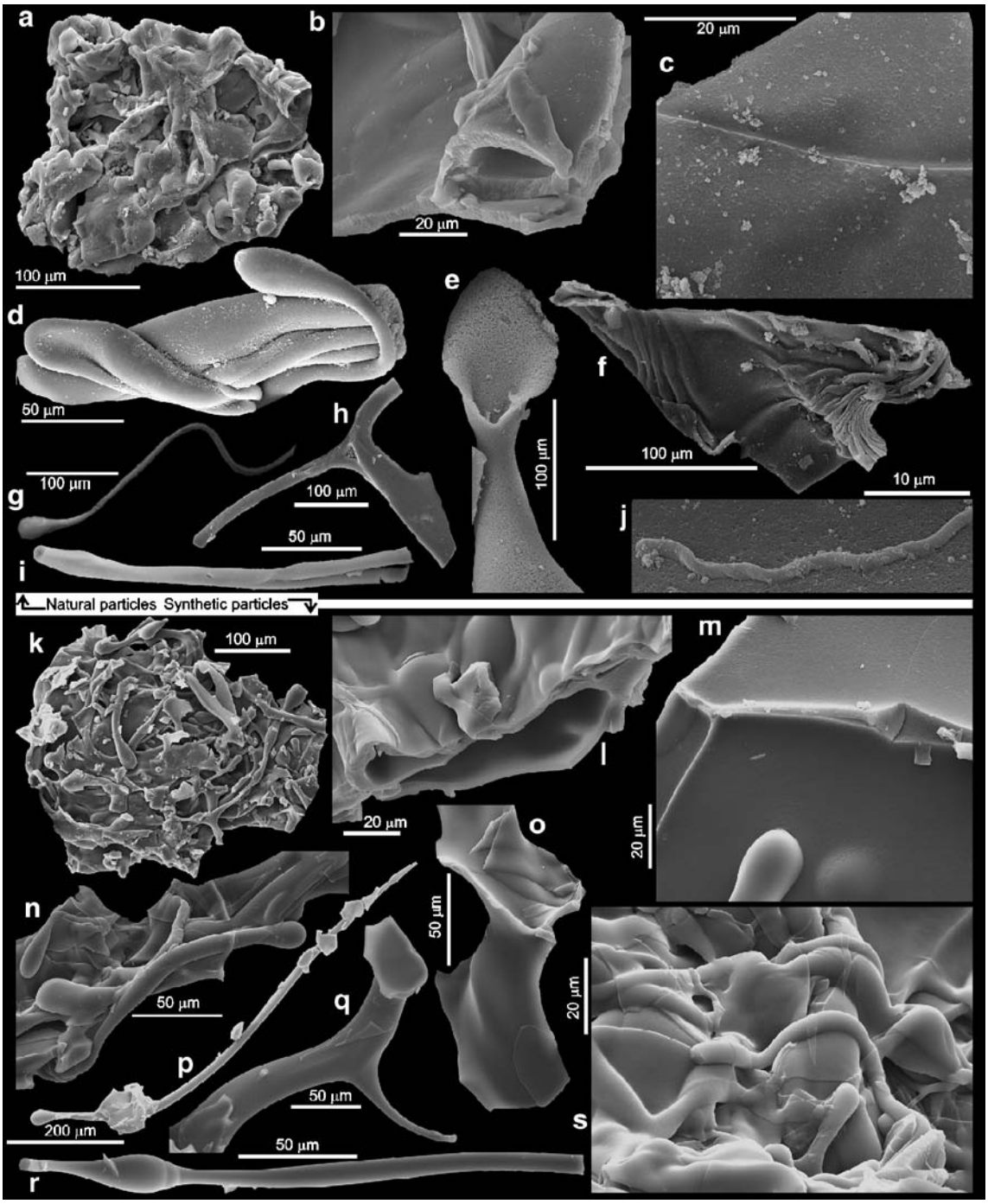


Fig. 2. Natural (a–j) and experimentally (k–s) produced cryogenic silica particles. Sheets (b, c, f, l, m) and threads (g, h, i, p, q, r) form the basic structures of particle morphology. Threads often exhibit branching (d, n), swellings (i, r) and are terminated by "tear-drops" (d, g, n, p). Sheets may also be folded (b, f, l) and branch (c, m). Combinations of these structures create funnels (e, o) and structurally complex particles (a, k). Probable silicified microbe on natural particle (j) and pseudofossil "microbe" (s) created by an opal-A thread draped over an experimentally produced particle surface.

and partially cemented and/or coalesced opal-A microspheres with diameters of ca. 100 nm-1 μm. At SEM resolution and in light microscopy particle-aggregates appeared internally homogeneous (e.g. fractured edges of Fig. 2b,l). Aggregate external morphology was diverse, encompassing sheets and folded/pleated sheets

(Fig. 2b,c,f,l,m), cylinders/threads and tapered threads (Fig. 2e,g–i,p–r), complex particles (Fig. 2a,d,k,n) and blocks/flakes. Tear-drop shaped terminations were a common feature associated with thread-like features (Fig. 2d,g,k,n,p), whilst others exhibited swellings, constrictions (Fig. 2i,r) and/or branching (Fig. 2h,q).

EDX microanalysis of natural aggregates revealed the presence of Si, O plus trace concentrations of Na and Cl and, sporadically, Ca, Zn and Hg. Carbon was not detected (Supplementary data Fig. 3b). Collapsed microbial filaments with a sparse/thin coating of opal-A microspheres (Fig. 2j), which did contain carbon, were distributed throughout the particulate sediment. Filamentous features on synthetic aggregate surfaces (Fig. 2s) displayed a remarkable resemblance to the partially fossilized microbes associated with natural particle-aggregates but lacked carbon.

## 4. Discussion

The particle morphologies produced experimentally by freezing of silica solutions replicate closely the shapes and morphological diversity observed in natural sediments. We propose that the observed morphologies are the product of cryogenic processes analogous to those reported from sea-ice formation and from investigations of freeze-gelation.

### *4.1. Salt-water ice formation and brine environments*

During sea-ice formation dissolved ions are excluded from growing ice crystals and become concentrated at the ice-water interface forming brine. As the ice-water interface advances formation of dendrites (sub-parallel projections of ice) creates brine filled channels. Bridges of ice between adjacent channels trap and isolate micrometric cells of brine. Further crystallisation at low temperatures (ca. −30 °C) reduces the volume of isolated cells, increasing brine concentration until it depresses the freezing point to a level which halts crystallisation. If however temperatures remain higher pores link up at crystal boundaries creating brine sheets, tubes and pockets [19] and veins which cross-cut crystals. Replicas of brine features, created by resin impregnation ([20] Figs. 3–7), reveal that freezing of saline fluid creates an array of mould morphologies including cylinders, sheets, spirals, tapering threads, teardrops and branched cylinders. Comparison of our natural and synthetic silica particles with photos of brine channels ([21] Fig. 1; [22] Fig. 2.2h), and resin casts of brine channels ([20] Figs. 3–7), suggest that the silica morphologies reported are the product of templating, moulding and casting within brine channels.

### *4.2. Cryogenic silica precipitation; a materials science perspective*

Cryochemical techniques have been employed in materials science to produce a spectrum of silica particle morphologies including fibres, flakes, ribbed flakes, sponges and honeycombs. Of relevance to this study is the process of freeze-gelation, in which silica-hydrosols, hydrogels or slurries are frozen. During freezing water partitions into ice crystals, whilst colloidal components are physically forced into diminishing interstitial sites. At the same time remaining silicic acid undergoes polymerization which favours particle cementation. Rapid freezing of silica sols produces sponge-like microstructures with interconnected networks of pores [23]. Unidirectional freezing of gelled aqueous silica creates elongate, parallel-sided ice crystals that have been used to create polygonal fibres, flakes and honeycombs with elongate macropores [23,24]. Silica concentrations utilized in these procedures (0.5–5 M $SiO_2$) are significantly greater than those encountered in hot springs, although unidirectional freezing of more dilute aged silicic acid (0.1–0.5 M $SiO_2$) has produced flakes and fibres with rounded and tapering cross-sections and occasional branching [24].

### *4.3. Opal-A deposition at sub-zero temperatures in geothermal environments*

The sub-zero winter air temperatures on the Yellowstone Plateau profoundly influence opal-A deposition (Fig. 3). As the erupted geothermal fluid cools opal-A initially nucleates and precipitates as described for summer deposition (Section 1.2; Fig. 3) until the temperature falls below the freezing point of water. Ice crystal formation then begins to remove solvent and partition dissolved species plus colloidal particles (as observed in sea-ice formation [22] and simulations of microbe incorporation into ice [25]) into residual pore fluid.

Ice formation has important chemical and physical consequences (Fig. 3). As fluids cool more rapidly than in summer they have less time in which “normal” processes of nucleation, particle growth and precipitation can operate and reach the freezing point whilst still supersaturated with opal-A. Freezing further increases the degree of supersaturation, promoting continued silica nucleation, polymerization and particle growth as the solvent is removed. Ice crystal formation may provide additional nucleation surfaces.

A further consequence of ice formation is a contemporary increase in the ionic strength of the residual

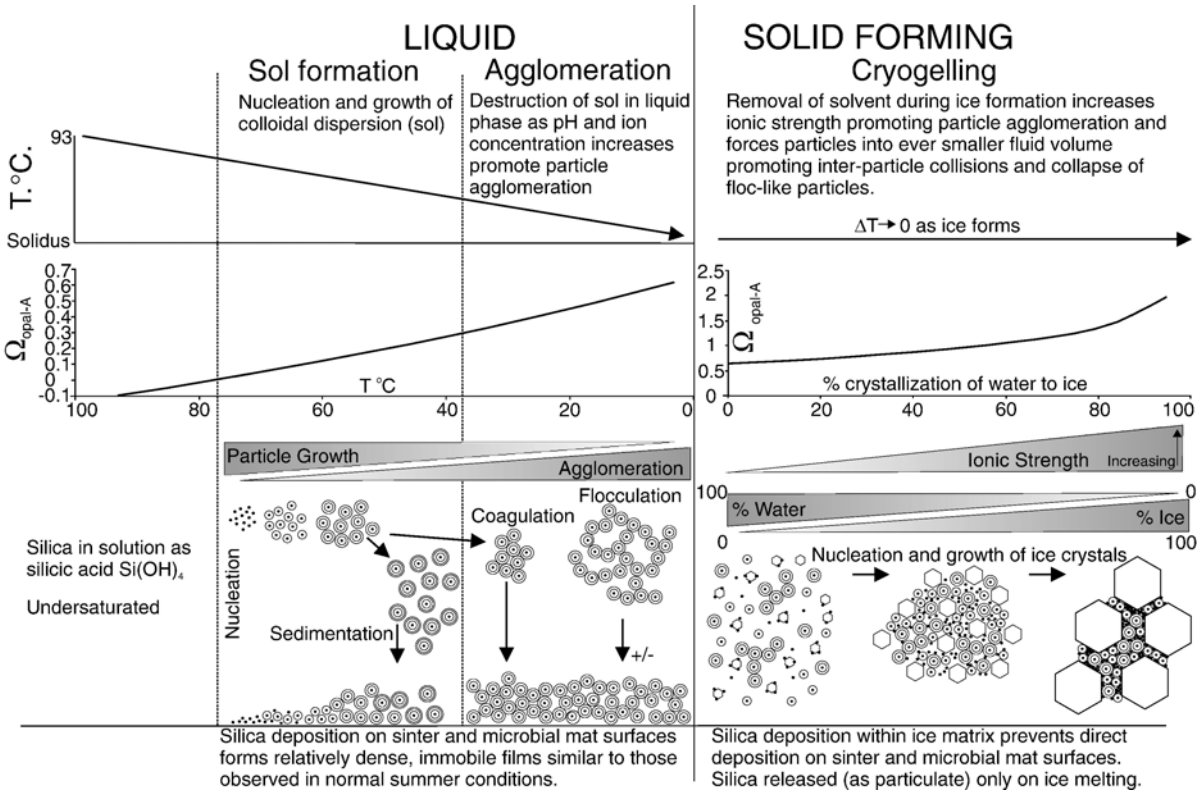


Fig. 3. Processes forming cryogenic silica morphologies in geothermal environments. The left hand side of the figure summarizes processes of opal-A precipitation at temperatures >0 °C. The right hand side of the figure summarizes processes occurring at temperatures of <0 °C when ice formation modifies solution chemistry and opal-A particle formation and agglomeration. Saturation indices ($\Omega_{\text{opal-A}}$, where $\Omega_{\text{opal-A}}=\log(\text{IAP}/K_{\text{sp}})$) are illustrative of processes and general chemical trends rather than being true chemical models of progressive changes in solution chemistry. Saturation index calculations utilize a typical Yellowstone geothermal fluid composition (see Section 1.2) and are calculated using MINEQL+ v 4.5. At $T>0$ °C $\Omega_{\text{opal-A}}$ is calculated on the basis that opal-A nucleation is suppressed. At T<0 °C $\Omega_{\text{opal-A}}$ is calculated for the case where opal-A nucleation is suppressed and where all solutes are partitioned in the aqueous residuum during freezing. Erupted fluid cools rapidly and becomes saturated with respect to opal-A below 80 °C. Initially opal-A nucleates and grows to form colloidal opal-A sols which may be destroyed by particle coagulation and flocculation. Silica formation under these conditions follows processes essentially identical to those active during summer conditions. The relative rates of opal-A nucleation versus the cooling rate of the geothermal fluid will ultimately control the extent of opal-A formation before freezing. Under these conditions, flocculated opal-A may sediment from solution to accumulate on sinter aprons, a process which may also continue below ice layers after freezing has begun. As the geothermal fluid is chilled to its freezing point, the formation of ice results in partitioning of both precipitated opal-A and aqueous solutes in the aqueous residuum. Solvent removal increases the ionic strength of the residual solution, promoting agglomeration and flocculation of opal-A particles and further nucleation of opal-A by i) concentrating remaining dissolved silica and ii) by nucleation of opal-A on ice crystal surfaces. Ongoing freezing increases the proportion of ice over liquid water and as ice crystals grow together opal-A precipitates become squeezed into and moulded by the shapes of the remaining brine channels into which they are partitioned, analogous to industrial cryogelling. On thawing, dilution of any remaining aqueous silica ensures that cryogenic silica is not cemented to sinter aprons but remains unconsolidated and is remobilized away from sinter aprons towards wetland environments.

solution, increasing the concentrations of ions such as Na, Ca, K, Mg, $HCO_3$ and $SO_4$. Many of these ions act as flocculants/coagulants in the presence of colloidal silica [26] and increasing ionic strength promotes opal-A particle aggregation. As freezing progresses particle aggregation is expected to become dominant over particle growth. In the early phases of freezing a combination of relatively high electrolyte concentrations and widespread particle dispersal in a liquid medium should favour the creation of open, floc-like silica aggregates. As ice formation continues a third process, the physical constriction of fluid environments, becomes important. Open aggregates are compressed by ice growth to produce dense aggregates. Dispersed silica microspheres are forced into an ever decreasing volume of fluid, physically forcing aggregate formation. Space restrictions impose dense packed configurations on microsphere aggregates (Fig. 3).

In the latter stages of freezing geothermal fluids are structurally similar to sea-ice and contain brine pockets

and veins. These features offer moulds, closely comparable in morphology and scale ([21] Fig. 1; [22] Fig. 2.2H; [20] Figs. 3–7) to the natural (Fig. 2a–j) and synthetic (Fig. 2k–s) opal-A particle-aggregates illustrated herein. The predominance, in sediments collected from beneath ice deposits, of dense aggregates over open floc-like morphologies is evidence of the importance of gelling in the latter stages of freezing.

Cyclic eruption patterns and diurnal temperature variations add complexity to precipitation pathways by creating cycles of thaw and refreezing, which remobilize and immobilize particles and aggregates. Many of the unusual particle-aggregate morphologies illustrated here could result from such cycles. Rucked/pleated sheets (Fig. 2f) could form during melting as silica particle-sheets possessing poor structural stability sit on inclined melting surfaces. Undulating or concave/convex sheets could result from draping of opal-A sediments over melted ice surfaces or the floors of melt water pockets. Fracturing of primary particle-aggregates during thawing and refreezing provides a mechanism for creating shard-like morphologies, a process that was replicated by subjecting experimental fluid containing particulate to a further cycle of thaw and freeze.

The preceding discussion concerns mainly eruptions from hot springs. Fluid erupted from geysers is often ejected in the form of an aerosol or droplets. In winter these freeze before hitting the ground. In such situations dissolved silica may be simply locked into the solid phase as dispersed particles. Alternatively, based on the evidence of large volumes of opal-A particulate in ice associated with Sawmill Geyser's ice cone, the processes of nucleation, polymerization and aggregation are accomplished with extreme rapidity.

### 4.4. Opal-A sediment trapping and remobilization

Rapid freezing of erupted vent fluid in winter curtails the "normal" summer silica deposition process. Accretion of silica to sinter aprons is halted in frozen environments because silica is locked within ice and isolated from sinter surfaces. Given a 4-month period of essentially uninterrupted sub-zero temperatures on the Yellowstone Plateau perhaps a third of the annual silica budget precipitated in the geothermal basins accumulates as unconsolidated precipitates within ice.

During winter substantial quantities of opal-A sediment accumulates on sinter aprons (e.g. Fig. 1c,d,j; Supplementary data Fig. 2c–e) because liquid water, required for sediment transport, freezes in all but the hottest environments. At Ear Spring, the low rate and broad/shallow pattern of discharge (Fig. 1b) caused ice and opal-A sediment formation and trapping only centimeters from the vent pool (Fig. 1a–c). During melting events remobilized sediment was trapped in small ice covered depressions formed behind microterrace dams on the sinter apron where it created millimeter-thick lenses (Fig. 1b). At Sawmill Geyser (Fig. 1f–h) ice cone formation trapped sediment where spray fell directly onto frozen substrates. Partial melting of the cone surface created small melt depressions that became localized collecting basins for opal-A particulate. In winter large-scale sediment transport is probably only possible over geothermally heated ground, in discharge systems of constantly erupting springs and during extremely high volume discharge events associated with sporadically erupting springs. Even in these circumstances transport distances appear to remain short as evidenced by sediment trapped below ice in a depression at Teakettle Spring (Supplementary data Fig. 2f,g) and melted from the ice cone of Saw Mill Geyser (Fig. 1j).

Sediment accumulated in winter remains unconsolidated as cementation is prevented by its incorporation in ice and by an apparent reduction in the influence of evaporation, a mechanism invoked in sinter sheet accretion [11]. Additionally cryogenic silica precipitation is near quantitative. On thawing, dilution precludes cementation to sinter aprons.

### 4.5. Recognition of cryogenic opal-A in hot spring sedimentary sequences

The recognition of cryogenic processes has implications for studies of sinter accumulation rates [9], the relative influence of biological and abiological controls on precipitate fabric [7,8] and biological versus abiological mass balance.

Following the spring melt, cryogenic sediment may be transported from sinter apron surfaces to areas of deposition, commonly shallow wetlands, by the resumption of "normal" hot spring or geyser discharge or heavy spring rains. Here, the sediment may form relatively thick and internally massive beds which can rapidly bury local vegetation [27]. The geothermally influenced wetlands of Yellowstone are environments of rapid diatomite accumulation [28]. At the outcrop and bed/laminae scale, diatomite and cryogenic sediments are likely to be indistinguishable. However, detailed investigations of wetland sedimentary sequences, in particular sediment particle morphology, should reveal annual influxes of cryogenic silica that, if sediments remain free of bio- and/or cryoturbation, will alternate with diatomite (e.g. [27]).

Sediment that remains trapped on sinter aprons following the spring melt can become fixed to apron surfaces as it dehydrates or is cemented by opal-A precipitation [27]. On exposed apron surfaces cryogenic sediment appears grainy and dull relative to the more vitreous opal-A deposited on similar surfaces directly from erupted fluids. Commonly, cryogenic sediment fills topographic depressions and drapes topographic highs (Fig. 1c c.f. [27] Fig. 4e). In vertical sections lenses of massive winter deposition, comprising granular opal-A particulate, will alternate with more vitreous and heterogeneous summer deposition comprising alternations of dense opal-A laminae with prostrate microbial filaments and porous laminae with *in situ*, in growth position microbes (e.g. [15] Fig. 14). The respective thickness of these interlayers is subject to the relative mass balance of winter versus summer opal-A deposition and sediment mobility following initial particulate accumulation. Additional features, indicative of unconsolidated sediments, may also provide evidence of the presence of cryogenic sedimentation, these include soft sediment deformation, desiccation structures and scours [27].

### 4.6. Wider implications

Cryogenic precipitation is not parochial to Yellowstone, initial observations indicate that cryogenic precipitates form at geothermal systems at high altitude (ca. 4200 m) at El Tatio, Chile and at high latitudes (ca. 65°N) at Geysir, Iceland. In addition to these silica dominated systems active salt/gypsum [29,30], carbonate [31] and iron [4,32] depositing springs occur in seasonally frozen environments. Palaeogeothermal areas may also have been subject to glaciations, however, these deposits will be troublesome to recognize due to diagenetic overprinting of primary textures.

Rapid mobilization and resedimentation of unconsolidated opal-A creates two mechanisms for fossil preservation. Firstly rapid sediment influxes bury local ecosystems, e.g. wetland vegetation [27] and low temperature microbial communities [33]. Secondly, freezing of geothermal fluids may act to partition and accumulate a formerly dispersed microbiota as has been reported for sea-ice brine networks [25,34–36] which would have a high potential for subsequent fossilization. Transport of such microfossil-rich sediment would allow thermophiles fossilized during the initial eruption-freezing process to be redistributed over broader areas, increasing the extent of biologically prospective hot spring environments.

Increasing evidence indicates the former presence of water on Mars [37,38]. Tectonism, volcanism and bolide impacts suggest that hydrothermal systems may have once been active [39–41] and interacted with sub-zero surface temperatures prompting analogy with winter conditions in Yellowstone. Given the presence of a Martian water-ice cryosphere [42], astrobiological investigation has been directed to cryophilic organisms [21], the stability of liquid water and life in frozen environments [22] and mineral spring-ice interactions [43]. On a cautionary note, we show that cryogenic particle formation, at least at silica geothermal springs, results in the formation of mineral structures which make convincing pseudofossils.

## 5. Conclusions

Sub-zero winter temperatures on the Yellowstone plateau promote rapid freezing of geothermal fluids and alter opal-A precipitation pathways resulting in cryogenic opal-A precipitation. This produces a range of unusual opal-A particle morphologies moulded within brine channels within ice. Sub-zero mean air temperatures between November and March on the Yellowstone Plateau mean that a significant proportion of the annual silica budget may be precipitated via a cryogenic mechanism. Despite extensive investigations of geothermal processes at Yellowstone, the importance of this silica formation mechanism has not been previously recognized. Cryogenic opal-A precipitation is expected to be a significant process at all modern and ancient eruptive geothermal systems influenced by sub-zero temperatures and freezing of erupted fluids.

## Acknowledgements

We thank Carolyn Davies, Jen Whipple, Smokey Sturtevant, Bill Wise and the staff of Yellowstone National Park. This research was supported through a NERC studentship grant and by the Leverhulme Trust, Grant F/00 407/S (A.C.) and Special Research Fellowship SRF/2000/0246 (I.B.).

## Appendix A. Supplementary data

Supplementary data associated with this article can be found, in the online version, at doi:10.1016/j.epsl.2007.02.026.

## References

[1] M.R. Walter, D. DesMarais, J.D. Farmer, N.W. Hinman, Lithofacies and biofacies of mid-Paleozoic thermal spring deposits in the Drummond Basin, Queensland, Australia, Palaios 11 (1996) 497–518.

[2] M.R. Walter, S. McLoughlin, A.N. Drinnan, J.D. Farmer, Palaeontology of Devonian thermal spring deposits, Drummond Basin, Australia, Alcheringa 22 (1998) 285–314.
[3] M.R. Walter, D.J. DesMarais, Preservation of biological information in thermal spring deposits: developing a strategy for the search for fossil life on Mars, Icarus 101 (1993) 129–143.
[4] M.L. Wade, D.G. Agresti, T.J. Wdowiak, L.P. Amendarez, J.D. Farmer, A Mossbaur investigation of iron rich terrestrial hydrothermal vent systems: lessons for Mars exploration, J. Geophys. Res. 104 (1999) 8489–8507.
[5] J.L. Bishop, E. Murad, M.D. Lane, R.L. Mancinelli, Multiple techniques for mineral identification on Mars: a study of hydrothermal rocks as potential analogues for astrobiology sites on Mars, Icarus 169 (2004) 311–323.
[6] S.L. Cady, J.D. Farmer, Fossilization processes in siliceous thermal springs: trends in preservation along the thermal gradient, in: G.R. Bock, J. Goode (Eds.), Evolution of Hydrothermal Ecosystems on Earth (and Mars?), Ciba Foundation Symposium, vol. 202, 1996, pp. 150–173.
[7] S.A. Guidry, H.S. Chafetz, Anatomy of siliceous hot springs: examples from Yellowstone National Park, Wyoming, U.S.A. Sediment. Geol. 157 (2003) 71–106.
[8] S.A. Guidry, H.S. Chafetz, Siliceous shrubs in hot springs from Yellowstone National Park, Wyoming, U.S.A. Can. J. Earth Sci. 40 (2003) 1571–1583.
[9] N.W. Hinman, R.F. Lindstrom, Seasonal changes in silica deposition in hot spring systems, Chem. Geol. 132 (1996) 237–246.
[10] D.E. White, R.A. Hutchinson, T.E.C. Keith, The geology and remarkable thermal activity of Norris Geyser Basin, Yellowstone National Park, Wyoming, USGS Professional Paper, vol. 1456, 1988, pp. 1–84.
[11] J.D. Rimstidt, D.R. Cole, Geothermal Mineralization 1: the mechanism of formation of the Beowawe, Nevada, siliceous sinter deposit, Am. J. Sci. 283 (1983) 861–875.
[12] S. Ohsawa, T. Kawamura, N. Takamatsu, Y. Yusa, Rayleigh scattering by aqueous colloidal silica as a cause for the blue colour of hydrothermal water, J. Volcanol. Geotherm. Res. 113 (2002) 49–60.
[13] H.E. Bergna, Colloid chemistry of silica: an overview, in: H.E. Bergna (Ed.), The Colloid Chemistry of Silica, American Chemical Society, Advances in Chemistry Series, vol. 234, 1994, pp. 1–47.
[14] S.A. Guidry, H.S. Chafetz, Depositional facies and diagenetic alteration in a relict siliceous hot spring accumulation: examples from Yellowstone National Park, U.S.A. J. Sediment. Res. 73 (2003) 806–823.
[15] B. Jones, R.W. Renaut, Hot spring and geyser sinters: the integrated product of precipitation, replacement and deposition, Can. J. Earth Sci. 40 (2003) 1549–1569.
[16] J.W. Ball, D.K. Nordstrom, R.B. McKleskey, M.A.A. Schoonen, Y. Xu, Water-chemistry and on-site sulfur-speciation data for selected springs in Yellowstone National Park, Wyoming, 1996–1998, US. Geological Survey, Open-file Report 01–49, 2001.
[17] C. Schreier, A Field Guide to Yellowstone's Geysers, Hot Springs and Fumaroles, Homestead Publishing, Moose, Wyoming, U.S.A., 1999, p. 128.
[18] N.R. Herdianita, P.R.L. Browne, K.A. Rodgers, K.A. Campbell, Mineralogical and textural changes accompanying ageing of silica sinter, Miner. Depos. 35 (2000) 48–62.
[19] B. Light, G.A. Maykut, T.C. Grenfell, Effects of temperature on the microstructure of first-year Arctic sea ice, J. Geophys. Res. 108 (2003) 1–16.
[20] J. Weissenberger, G. Dieckmann, R. Gradinger, M. Spindler, Sea ice: a cast technique to examine and analyze brine pockets and channel structure, Limnol. Oceanogr. 37 (1992) 179–183.
[21] J.W. Deming, Psychrophiles and polar regions, Curr. Opin. Microbiol. 5 (2002) 301–309.
[22] H. Eicken, From the microscopic to the macroscopic to the regional scale: growth, microstructure and properties of sea ice, in: T.D. Dieckmann, G.S. Dieckmann (Eds.), Sea Ice—an Introduction to its Physics, Biology, Chemistry and Geology, Blackwell Science, London, 2003, pp. 22–81.
[23] S.R. Mukai, H. Nishihara, H. Tamon, Formation of monolithic silica gel microhoneycombs (SMHs) using pseudosteady state growth of microstructural ice crystals, Chem. Commun. 7 (2004) 874–875.
[24] W. Mahler, M.F. Bechtold, Freeze-formed silica fibres, Nature 285 (1980) 27–28.
[25] H.M. Mader, M.E. Pettitt, J.L. Wadham, E.W. Wolff, R.J. Parks, Life in subsurface ice, Geology 34 (2006) 169–172.
[26] L.A. Williams, D.A. Crerar, Silica diagenesis II. General mechanisms, J. Sediment. Petrol. 55 (1985) 0312–0321.
[27] A. Channing, D. Edwards, S. Sturtevant, A geothermally influenced wetland containing unconsolidated geochemical sediments, Can. J. Earth Sci. 41 (2004) 809–827.
[28] L.J.P. Muffler, D.E. White, M.H. Beeson, A.H. Truesdell, Geological map of Upper Geyser Basin Yellowstone National Park, Wyoming. US. Geological Survey, Miscellaneous Investigations Series, Map-I 1371, 1982.
[29] J.L. Heldmann, W.H. Pollard, C.P. McKay, D.T. Andersen, O.B. Toon, Annual development cycle of an icing deposit and associated perennial spring activity on Axel Heiberg Island, Canadian high Arctic, Arct. Antarct. Alp. Res. 3 (2005) 127–135.
[30] W.H. Pollard, Icing processes associated with high Arctic perennial springs, Axel Heiberg Island, Nunavut, Canada, Permafr. Periglac. Process. 16 (2005) 51–68.
[31] Ø. Hammer, B. Jamtveit, L.G. Benning, D.K. Dysthe, Evolution of fluid chemistry during travertine formation in the Troll thermal springs, Svalbard, Norway, Geofluids 5 (2005) 140–150.
[32] B.K. Pierson, M.N. Parenteau, Phototrophs in high iron microbial mats: microstructure of mats in iron-depositing hot springs, FEMS Microbiol. Ecol. 32 (2000) 181–196.
[33] N.H. Trewin, S.R. Fayers, R. Kelman, Subaqueous silicification of the contents of small ponds in an Early Devonian hot spring complex, Rhynie, Scotland, Can. J. Earth Sci. 40 (2003) 1697–1712.
[34] B.P. Price, A habitat for Psychrophiles in deep Antarctic ice, Proc. Natl. Acad. Sci. 97 (2000) 1247–1251.
[35] K. Junge, H. Eiken, J.W. Deming, Bacterial activity at −2 to −20 °C in Arctic wintertime sea ice, Appl. Environ. Microbiol. 70 (2004) 550–557.
[36] C. Krembs, H. Eiken, K. Junge, J.W. Deming, High concentrations of exopolymeric substances in Arctic winter ice: implications for the polar ocean carbon cycle and cryoprotection of diatoms, Deep-sea Res. I 49 (2002) 2163–2181.
[37] J.-P. Bibring, Y. Langevin, F. Poulet, A. Gendrin, B. Gondet, M. Berthe, A. Souflott, P. Drossart, M. Combes, G. Bellucci, V. Moroz, N. Mangold, B. Schmitt, the OMEGA team, Perennial water-ice identified in the south polar caps of Mars, Nature 428 (2004) 627–630.
[38] R.L. Mancinelli, T.F. Fahlen, R. Landheim, M.R. Klovstad, Brines and evaporites: analogs for Martian life, Adv. Space Res. 33 (2004) 1244–1246.
[39] J.D. Farmer, Hydrothermal systems on Mars: an assessment of present evidence, in: G.R. Bock, J. Goode (Eds.), Evolution of

Hydrothermal Ecosystems on Earth (and Mars?), Ciba Foundation Symposium, vol. 202, 1996, pp. 273–295.
[40] E.S. Varnes, B.M. Jakosky, T.M. McCollom, Biological potential of Martian hydrothermal systems, Astrobiology 3 (2003) 407–414.
[41] F. Pirajno, M.J. Van Kranendonk, Review of hydrothermal processes and systems on Earth and implications for Martian analogues, Aust. J. Earth Sci. 52 (2005) 329–351.
[42] M.B. Wyatt, H.Y. McSween, K.L. Tanaka, J.W. Head, Global geologic context for rock types and surface alteration on Mars, Geology 32 (2004) 645–648.
[43] S. Grasby, C.C. Allen, T. Longazo, J.T. Lisle, D.W. Griffin, B. Beauchamp, Supraglacial sulfur springs and associated biological activity in the Canadian High Arctic—signs of life beneath the ice, Astrobiology 3 (2003) 583–596.